Journal of Applied Geophysics 196 (2022) 104511

Contents lists available at ScienceDirect

Journal of Applied Geophysics

journal homepage: www.elsevier.com/locate/jappgeo

Joint inversion of airborne TEM data and surface geoelectrical data. The Egebjerg case

Niels B. Christensen

Department of Earth Sciences, University of Aarhus, Hoegh Guldbergsgade 1, 8000 Aarhus C, Denmark

ARTICLE INFO

Keywords:
Geoelectrical
Electromagnetic
Joint inversion

ABSTRACT

In modern hydrogeological investigations with dense data coverage, the aim is to combine several different sources of information about subsurface structures to enable the best possible geological and hydrogeological interpretations from which a dynamic hydraulic model can be constructed. In this paper, the Egebjerg area in Denmark is used as an example of the process of combining airborne transient electromagnetic data with ground-based galvanic geoelectrical data in a joint inversion to produce a better resolution of the subsurface resistivity structure than would be possible using each of the methods alone. The joint inversion is realised by mutually constraining the inversion models of one data set with the inversion models of the other, overcoming the differences in scale and resolution power that are inherent in this type of effort.

1. Introduction

A well established guideline in modern geophysical investigations is to integrate as many different sources of information as possible in the interpretation process to increase the reliability of the results: different types of geophysical data, prior geological information, surface observations, satellite data, etc. In this endeavour, jointly inverting different types of geophysical data in a survey area, if available, becomes an important part, and the literature is full of examples of methodologies and practical examples. The essential goal of joint inversion is to produce a model that has a better resolution of the subsurface resistivity than would be obtainable from individual inversion of the two methods. This goal can be realised because the two methods might have different scale lengths of sensitivity, e.g. different depths of penetration and thereby supplement each other to obtain a better depth coverage. In other cases, the two methods inherently have different resolution properties such as galvanic and inductive data where a combination may help resolve the equivalences met in either method. The latter is the subject of Sharma and Verma (2011).

An example of joint inversion of the same data types from different instruments is found in Triantafilis et al. (2011), where data from two different ground conductivity meter (GCM) instruments are jointly inverted.

In Haroon et al. (2015), data from ground based long-offset transient electromagnetic (TEM) and ground based central loop TEM configurations are jointly inverted in an investigation of a mud volcano in Azerbaijan. The long-offset TEM method has a deep penetration, while the other: ground based central loop TEM data, has a better near-surface resolution. A combination of airborne frequency domain data with ground based TEM and frequency domain RMT data is presented in Sudha and Siemon (2014) exploring the Cuxhaven valley, Germany.

In all of the examples of the previous paragraph, the methods involved are inductive and thereby sensitive to the horizontal resistivity, so there is no immediate problem in combining them. However, many of the published cases of joint inversion involve a combination of inductive data being sensitive to the horizontal resistivity and galvanic data being sensitive to the geometrical mean of the horizontal and vertical resistivities. One of the earliest examples is published in Vozoff and Jupp (1975) who combine magnetotelluric (MT) and DC geoelectrical data. Examples of combining TEM data with DC geoelectrical data are found in Christiansen et al. (2007), Fernando and Hesham (2010), and in Albouy et al. (2001) who use the joint inversion to map coastal aquifers.

The issues raised by the fact that DC geoelectrical and inductive data are sensitive to different measures of subsurface resistivity is addressed in Meju (2005), and Christensen (2000) addresses the subject by investigating the concept of anisotropy and how well it may be resolved.

This paper explores the potential of joint inversion of airborne and ground based data with a field example from the Egebjerg area, eastern Jutland, Denmark, where airborne TEM data were collected by the SkyTEM system (Sørensen and Auken, 2004) and ground based geoelectrical data were measured with the Pulled Array Continuous Electrical Sounding (PACES) system (Sørensen, 1996). The methodology is a

E-mail address: nbc@geo.au.dk.

https://doi.org/10.1016/j.jappgeo.2021.104511
Received 16 August 2021; Received in revised form 8 November 2021; Accepted 25 November 2021
Available online 3 December 2021

combination of a standard iterative least squares inversion procedure (Christensen, 2016b) and the Lateral Parameter Correlation (LPC) approach (Christensen, 2016a). Two issues, to be addressed in the following, arise in the combination of these methods: a depth scale issue and the well known issue of combining inductive and galvanic data which are sensitive to different resistivity measures.

The issue of scale arises in many situations of joint/cooperative inversion and it is rather the norm than the exception. An extreme example is the inclusion of borehole log information in EM inversion: The effective volume of the sensitivity function of borehole data is often many orders of magnitude smaller that the volume occupied by the EM sensitivity. The log information rarely extends beyond a fraction of a meter from the borehole axis, and it stops quite abruptly at the bottom of the log. A conceptually consistent way of integrating borehole log information in surface or airborne EM inversion is presented in Christensen and Lawrie (2018).

An example where the scale differences are similar to the ones in this paper - and where consequently the approach presented here might have some relevance - is the joint inversion of airborne frequency and time domain data, where the frequency domain data would have a penetration depth of 50–70 m while that of the TEM data would often be 100 s of meters. Yet another example is the still more extensive use of ground conductivity meters (GCM) and attempts to jointly invert this frequency domain data type with a fairly shallow penetration with e.g. TEM data of various kinds. In these cases, the subsurface parameter in question is the same: the horizontal resistivity.

The issue of jointly inverting related, but not identical resistivity measures, as in the present case, arises in the many examples of jointly inverting geoelectrical data and inductive data as mentioned above. In some cases, this challenge is acknowledged, but certainly not always.

In other joint inversion efforts, where the parameters are uncorrelated as in seismic slowness and EM resistivity, the structure rather than the bulk parameter is what correlates the two methods. In this case, correlation can be expressed through cross-gradient constraints, but that is beyond the scope of this paper.

The methods and approaches presented in this paper are relevant in other cases of combining different electromagnetic data, but in each case, inverters and interpreters will have to analyse the specifics of their own situation and find appropriate approaches.

2. The EGEBJERG survey area

The Egebjerg study area is situated in Jutland, Denmark, north of the town of Horsens, see Fig. 1. The survey area covers ~145 km^2 and the geophysical investigations were carried out as part of the National Groundwater Mapping project, the aim of which is to map the important aquifers in Denmark with a dense net of geophysical and other measurements with the aim of improving geological and hydrogeological modelling and to set up dynamic hydraulic models to support a long term sustainable abstraction of groundwater. The area is dominated by Quaternary sediments of clay and sand with several buried valleys eroded into in the pre-Quaternary surface by repeated glaciation events. The most important aquifers in the area used in abstraction of groundwater are predominantly situated in the buried valleys in sandy and gravelly sediments (Jørgensen et al., 2010).

In the area, mainly two geophysical data sets were collected: An airborne TEM survey conducted with the SkyTEM system (Sørensen and Auken, 2004) in April–May 2007, and ground-based, measure-while-moving Pulled Array Continuous Electrical Sounding method (PACES) (Sørensen, 1996). The TEM survey comprises 625 km of production data processed to be located at 23,695 positions. All of the data post processing: stacking, averaging and filtering was done in the WorkBench (WB) shortly after the survey was conducted (Auken et al., 2015). The PACES data were collected along lines in five different subareas, not systematically coinciding with the TEM flight lines and comprise ~28,000 sounding positions. Fig. 1 shows a map of the survey area indicating the positions of the TEM and PACES measurements. After the survey, according to Danish regulations, data including information about the processing and the inversion results were stored in the national geophysical data base, GERDA, from which they were retrieved for this project.

The Egebjerg area is densely populated with many man-made infrastructure elements, such as roads, power lines, buried cables, fences, etc. that are often the source of cultural coupling phenomena in the inductive TEM data. An important element of the data processing is therefore to identify and cull the disturbed TEM soundings which leaves 'holes' in the TEM data coverage (see Fig. 1). This resulted in ~30% of the original soundings being culled, leaving 23,695 sounding positions available for inversion.

Boreholes are sparsely distributed in the area, and lithological information was only available from about half of them. A handful of boreholes were logged with electrical logs, but were also so sparsely distributed that they have not been included in the inversions presented in this paper. However, the information that could be gleaned from the boreholes was of course included in subsequent geological/hydrogeological interpretation of the inversion results.

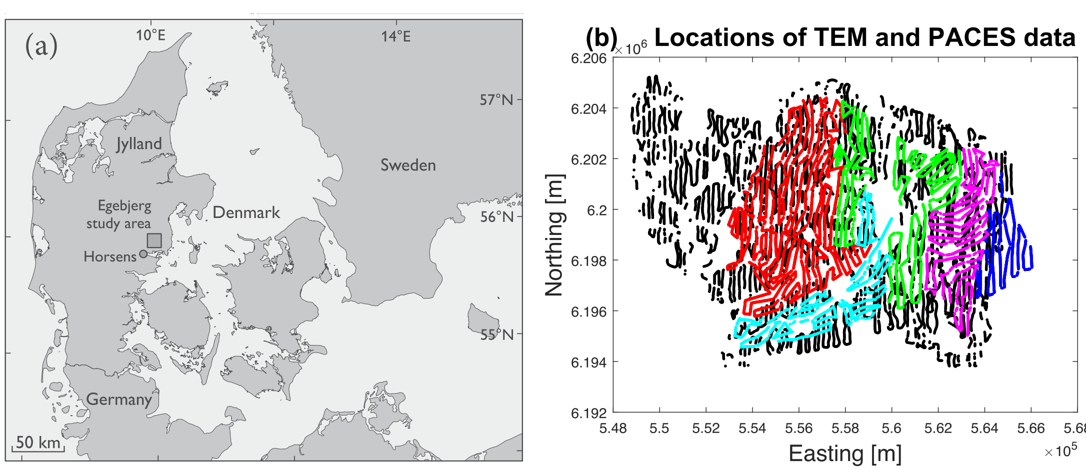

Fig. 1. (a): The location of the Egebjerg survey area in eastern Jutland, Denmark. (b): The Egebjerg survey area with SkyTEM lines in black and the five PACES surveys in blue, red, green, cyan, and magenta.

3. The data

3.1. The SkyTEM airborne data

The SkyTEM data were collected with a dual moment system consisting of a low moment (LM) and high moment (HM). LM data are measured with a smaller transmitter (Tx) moment with a short turn-off time that permits early gates to be measured and which can thereby provide information about the shallow subsurface. HM data are measured with a large Tx moment with a longer turn-off time that gives a larger signal-to-noise level at late delay times and which can thereby provide information about the deeper subsurface. LM data are recorded in 19 gates spanning gate centre times from$\sim$17μs to 1.1 ms, while the HM data are recorded in 23 gates spanning gate centre times from$\sim$58μs to 8.8 ms. I is seen that there is a fairly wide overlap between the two moments.

The LM and HM Tx waveform had to be retrieved from plots in the original reports, using an open-source digitising program: https://apps.automeris.io/wpd/ and subsequently reducing the samples to a best fitting piecewise linear waveform. The repetition frequency for the LM data is 222.22 HZ with an ontime of 800μs and a turnoff time of$\sim$11.8μs. The repetition frequency for the HM moment, was 25 Hz with an ontime of 10 ms and a turnoff time of 43μs. The receiver (Rx) cutoff frequency was 450 kHz as a second order filter, while the cutoff frequency of the amplification system was 106 kHZ as a first order filter. LM data were recorded with a front gate time of 11.5μs while the HM data were recorded with a front gate of 47.5μs.

3.2. TEM data post-processing procedures

As mentioned, the original data processing was performed in the WB program (Auken et al., 2015) and subsequently uploaded to the GERDA data base. The data files retrieved from GERDA contained information about data values, V, and an estimate of the relative data noise, ΔV_{rel}^{data}. The total relative noise is found as the sum of contributions from the absolute noise and an ad hoc relative noise to account for the unknown data errors and errors connected with the approximate nature of using a 1D model in the inversion. The overall relative noise level is then given as:

$$\Delta V_{rel}^{total} = \sqrt{0.03^2 + \left(\Delta V_{rel}^{data}\right)^2} \tag{1}$$

In principle, all of the data were used in the inversion. However, the WB data file contains LM and HM data at different positions for each. I have combined LM and HM data in my input data files by combining every LM sounding with the closest HM sounding. This resulted in $\sim$11,300 sounding positions. Finally a selection criterion was implemented stating that the distance between LM and HM data locations must be smaller than 20 m and that if no HM sounding was found within 20 m, the data set was culled. This resulted in a total number of $\sim$11,000 full soundings. The limiting value of 20 m was arrived at by looking at the distribution of smallest distances between a LM and HM sounding, see Fig. 2.

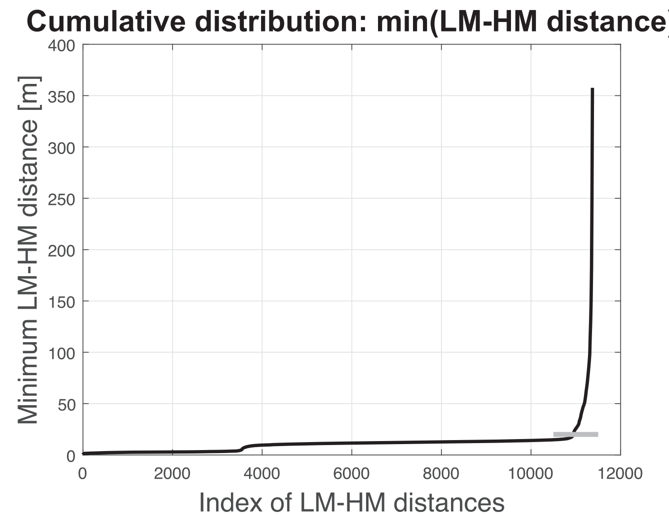

Fig. 2. Cumulative distribution of minimum LM-HM distances in the Egebjerg data set. The limiting value of 20 m is indicated with a short gray line.

3.3. The PACES data

Beside the TEM survey conducted in the Egebjerg area in 2007, five Pulled Array Continuous Electrical Sounding (PACES) surveys (Sørensen, 1996; Rambøll, 2011) were carried out in subareas of the Egebjerg area (see Fig. 1). The surveys were conducted with the aim of performing a detailed investigation of the near-surface geology, mainly to find the distribution of near-surface clays and sands. The five surveys were carried out at different times with three slightly different PACES electrode arrays. All PACES electrode arrays have the same nominal electrode configuration, see Fig. 3, but due to the manufacturing process they can differ slightly from each other. The five surveys yield a total of 28,000 sounding positions. Data processing consisting in interpolation of each of the electrode configuration to a common midpoint for the lateral sensitivity function of each of the configurations plus some filtering was carried out in the WB program before being uploaded to GERDA. I have used the PACES data as-is ascribing a uniform relative noise of 5% to all data.

4. Inversion

4.1. Inversion formulation

The inversion approach used in this paper is a well-established iterative damped least squares approach (Menke, 1989). The model update at the n'th iteration is given by

$$m_{n+1} = m_n + \left[G_n^T C_{obs}^{-1} G_n + \frac{1}{\sigma_v^2} C_m^{-1}\right]^{-1} \cdot$$

$$\left[G_n^T C_{obs}^{-1}(d_{obs} - g(m_n)) + C_m^{-1}(m_{prior} - m_n)\right] \tag{2}$$

where m is the model vector containing the logarithm of the model parameters, G is the Jacobian matrix containing the derivatives of the data with respect to the model parameters, T indicates matrix transpose, C_m is a model covariance matrix imposing a vertical smoothness constraint on multi-layer models, σ_v is the standard deviation of C_m, C_{obs} is the data error covariance matrix, d_{obs} is the field data vector, $g(m_n)$ is the nonlinear forward response vector of the n'th model. In this study, as is most often the case, the data noise is assumed to be uncorrelated, implying that C_{obs} is a diagonal matrix. It would be desirable to include a full data error covariance matrix, but unfortunately this is not possible as I have no access to the raw TEM or PACES data. Likewise, a proper modelling error covariance matrix would improve the inversion as illustrated in Bai et al. (2021).

The model parameter uncertainty estimate is based on a linear approximation to the posterior covariance matrix, C_{est}, given by

$$C_{est} = \left[G^T C_{obs}^{-1} G + \frac{1}{\sigma_v^2} C_m^{-1}\right]^{-1}$$

where G is based on the model achieved after the last iteration. The analysis is expressed through the standard deviations of the model parameters obtained as the square root of the diagonal elements of C_{est} (e.g. Inman Jr. et al., 1975).

The model covariance function, C_m, is chosen as a broad-band von

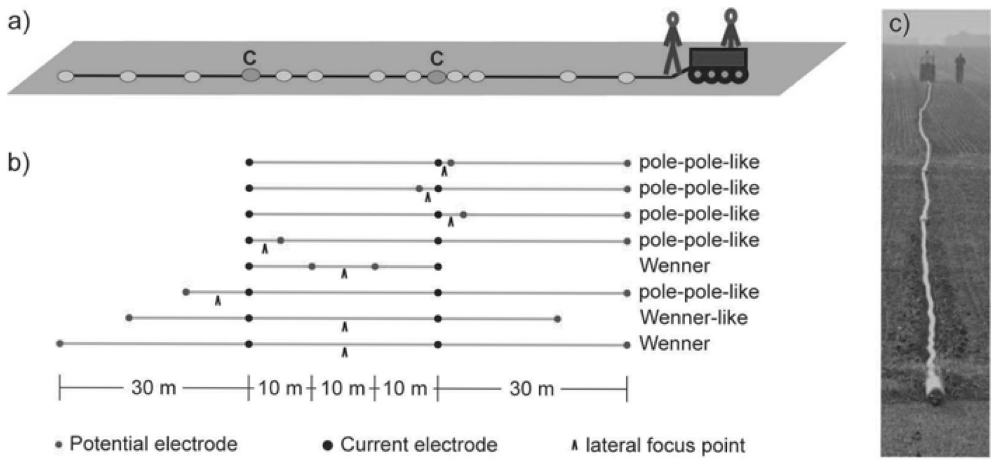

Fig. 3. (a): The PACES system. The current electrodes are marked with a 'c'. (b): The PACES electrode configurations. (c): A photo of the system operating in the field.

Karman covariance function containing essentially all correlation lengths, and it is used for its superior robustness. For details see Serban and Jacobsen (2001), Christensen and Tølbøll (2009), and Maurer et al. (1998).

4.2. The model

The model used in the inversions is a one-dimensional (1D) 35-layer multi-layer model (MLM) consisting of horizontal, homogeneous and isotropic layers. To simplify the correlation between the models obtained in the inversion of both TEM and PACES data, the model discretisation is chosen so that the model accommodates the resolution properties of both types of data. The top layer is 0.5 m thick to reflect the near-surface resolution properties of the PACES data, and the depth to the bottom layer is 400 m which covers the depth resolution of the TEM data. The initial/prior model for the TEM data has a resistivity of 70 Ohmm in the top layer increasing to 200 Ohmm in the bottom layer. Experience shows that this is good and robust starting model for TEM data. It is conductive enough to produce a non-vanishing response, and the higher resistivity with depth ensures that the responses of the first iterations - and thereby the derivatives with respect to layer resistivity - actually sample the bottom of the model. PACES inversions are less critical with respect to the initial model, so the same model is used in the inversion of the PACES data.

Present inversion options with commercially available software include multidimensional inversion of the PACES data, but not for the TEM data. However, a joint inversion with 1D TEM models and 2D/3D PACES models would present additional conceptual complexities, and to avoid these, both data sets have been inverted with a 1D approach.

4.3. Inversion strategy

The aim of the inversion efforts is to produce three models of the survey area: One using only the TEM data; one using only the PACES data; and a joint inversion of both data sets. The individual inversions will be conducted through the following steps (Christensen, 2016a; Christensen, 2016b):

(1) An inversion with the initial/prior 35-layer MLM as mentioned above and with the same vertical constraints for consistency is carried out (Christensen, 2016b). This produces the uncorrelated inversion result.
(2) Then the Lateral Parameter Correlation (LPC) procedure is used to implement a lateral correlation in the plane (2D) of the uncorrelated models from the initial inversions (Christensen and Tølbøll, 2009; Christensen, 2016a).
(3) The correlated models are then used as prior models for a final individual inversion with the posterior uncertainties of the LPC procedure as constraints on the individual layer parameters. This produces the final laterally correlated inversion result.

After both data sets have been inverted in this way, a joint inversion of the two data sets is produced by:

(4) Lateral 2D correlation of all uncorrelated TEM and PACES models. This permits all models to influence each other according to their uncertainty and mutual distance.
(5) The correlated model results are then used as prior models for a final separate inversion of the individual TEM and PACES data sets with the posterior uncertainties of the LPC procedure as constraints on the individual layer parameters. This produces the joint/co-correlated inversion results.

This is the overall plan for the inversions. However, two issues need to be addressed. First of all, the two data sets have quite different depth ranges of resolution, and the weights with which the two methods enter in the LPC procedure need to reflect this. Secondly, correlating an inductive and a galvanic data set must take into account that TEM data, being inductive, reflect the horizontal subsurface resistivity while the PACES data, being galvanic in nature, reflect the geometric mean of the vertical and horizontal resistivity. To meet the aim of improving the near-surface resolution of the TEM models by a joint inversion, these issues must be addressed. More about this in the following sections.

5. Inversion results

In the following sections, the inversion results will be presented as selected model sections through the area. Neither the TEM data nor the PACES data retrieved from the GERDA data base refer to line/flight numbers, so the model sections presented here are obtained by interpolation of the inversion results from both data sets to NS lines using the Natural Neighbour method. The line distance is 200 m and the sample distance on the lines is 40 m, roughly the same as the minimum TEM sounding distance for the combined LM + HM soundings. After interpolation, the interpolated points outside of the convex hull of the original data were removed, and subsequently all interpolated positions with a minimum distance to an original data set more than 200 m were removed, resulting in 15,399 interpolated positions. Fig. 4 shows the locations of the original data and the selected interpolated positions for

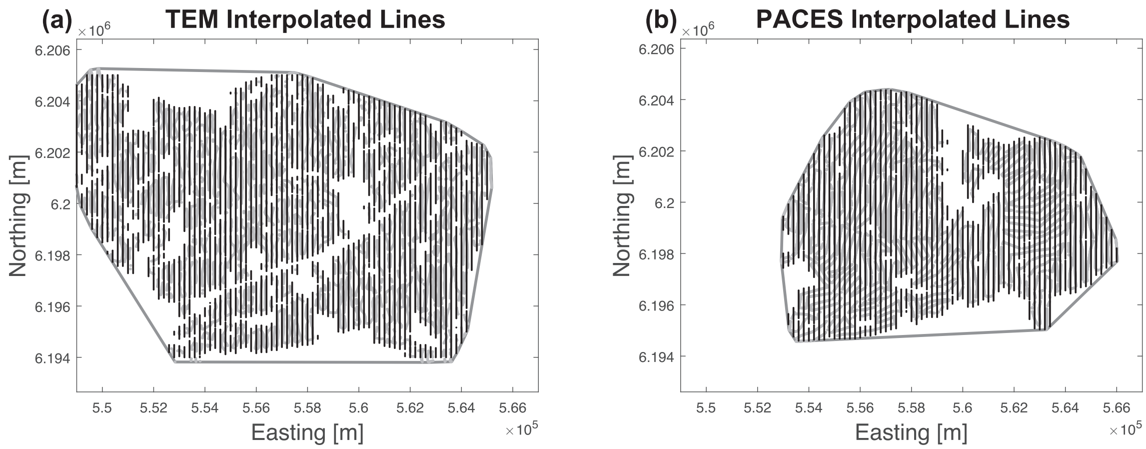

Fig. 4. (a): Locations of the original TEM data (gray dots) and the selected interpolated positions (black dots) in the Egebjerg survey area. The locations of the three lines shown in Figs. 5, 6 and 7 are indicated with arrows at the top of the plot. (b): Same for the PACES data.

both TEM and PACES data.

Because of the selection criteria and the culling of the culturally coupled data sets, many of the resulting TEM model sections have 'holes' in them of various sizes. Likewise for the PACES model sections: The 'holes' in the model sections indicate intervals where access was impossible because of infrastructure.

In the following, model sections were chosen mainly to illustrate one of the main purposes of the survey: To identify the buried valleys in the area where the important aquifers were most likely to be found. All of the models sections will show the laterally correlated inversion results for the individual inversions of the TEM and PACES data and for the joint inversion.

5.1. Inversion results of the TEM data only

Fig. 5 shows three model sections of the TEM inversion results from the central survey area indicating the presence of buried valleys. In the top and middle plot frames of Fig. 5, the buried valleys can be seen at Northing 6196,500 m and 6202,000 m, the northernmost of them the deepest with an aquifer with potentially more yield because the valley infill seems to be more resistive. In the lowermost plot frame of Fig. 5, both valleys have more or less disappeared. The three model sections also show the variability of the resistivity in the near-surface parts of the profile with alternating resistive and moderately conductive layers, geologically most likely to be sand and moraine clay lithologies, respectively. At the bottom of the model sections, resistivities are quite low, indicating the Tertiary heavy clays out of which the buried valleys have been eroded and which are known to be present in the area. This formation constitutes the hydraulic bottom of the aquifers. On line 100,042, resistivities seem to increase with depth below the Tertiary clay, but these model details are not reliable; they appear below the depth of information (DOI) indicated in all three plots. The DOI is defined as the maximum of the depths to the centroids of the absolute values of the rows of the model resolution matrix, see Christensen (2021).

5.2. Inversion results of the PACES data only

Fig. 6 shows model sections of the PACES inversion results for the same three lines as the TEM data in Fig. 5. Notice the change of scale. The DOI of the PACES inversions lies quite steadily at 25–30 m below surface, and it is obvious how there is no model resolution below this depth: The resistivities below~30 m are determined solely by the model covariance matrix of the vertical regularisation and the resistivities around a depth of~30 m. However, in the top 30 m, the PACES results show a better resolution of the details of the distribution of resistive and more conductive lithologies than the TEM results.

5.3. Joint inversion of the TEM and PACES data

Fig. 7 shows the model sections of the TEM models obtained through a joint TEM and PACES inversion for line 100,034. Comparing with the plots in Fig. 5, it is seen that the improved model resolution at the near-surface of the PACES models have influenced the models of the joint inversion - as was in fact the rationale behind the joint inversion efforts. The resistivities in the deeper parts of the model are pretty much the same as before - as they should be because the PACES data have no resolution at depth.

The model section for the joint inversion results of the PACES data also shown in Fig. 7 shows that the deeper parts of the model section are influenced mainly by the TEM models - as they should.

The results shown in Fig. 7 were only obtained after some modification of the joint inversion procedure. The predicted models from the LPC procedure are influenced by the standard deviation of the model parameters of the models included in the correlation, plus the mutual distances between the models scaled by a model correlation matrix. As seen in Fig. 6, the parts of the PACES models below the DOI are only governed by the vertical regularisation and the resistivity values just around the DOI. In fact there is no information in these characteristics, and they should not be allowed to influence the joint inversion result. To prevent this, the standard deviation of the PACES model parameters in the uncorrelated inversion below the DOI were multiplied with a factor increasing quite steeply with depth. For the first 19 layers, i.e. down to a depth of 34.13 m, the multiplication factor is 1, and for layers 20–35, the multiplication factor is chosen as $2^{(N-19)}$ where $N$is the layer number, but truncated at a maximum value of 999. For a discussion of the issues of weighting between the inversion results of different methods and data sets, see also Sudha and Siemon (2014).

In Fig. 7, model sections for line 100,034 show the joint inversion results of the TEM data, the joint inversion of the PACES data, and the joint inversion of the TEM data in case the down-weighting of the deeper parts of the PACES models are omitted. The latter clearly shows that the TEM models will be overly influenced by the deeper parts of the PACES models becoming more resistive than they should be. Comparing Figs. 6 and 7 it is clear that - as expected and as intended - the deeper parts of the models of the PACES joint inversion are now very similar to the TEM resistivity distribution.

The improved near-surface resolution of the TEM models from the joint inversions is illustrated in Fig. 8 which shows the resistivity of layer 10 in the depth interval 6.28 -7.52 m. In the western parts of the survey area there is little difference while the resistivity distribution displays a more complex, and more resistive, picture for the joint inversions in the

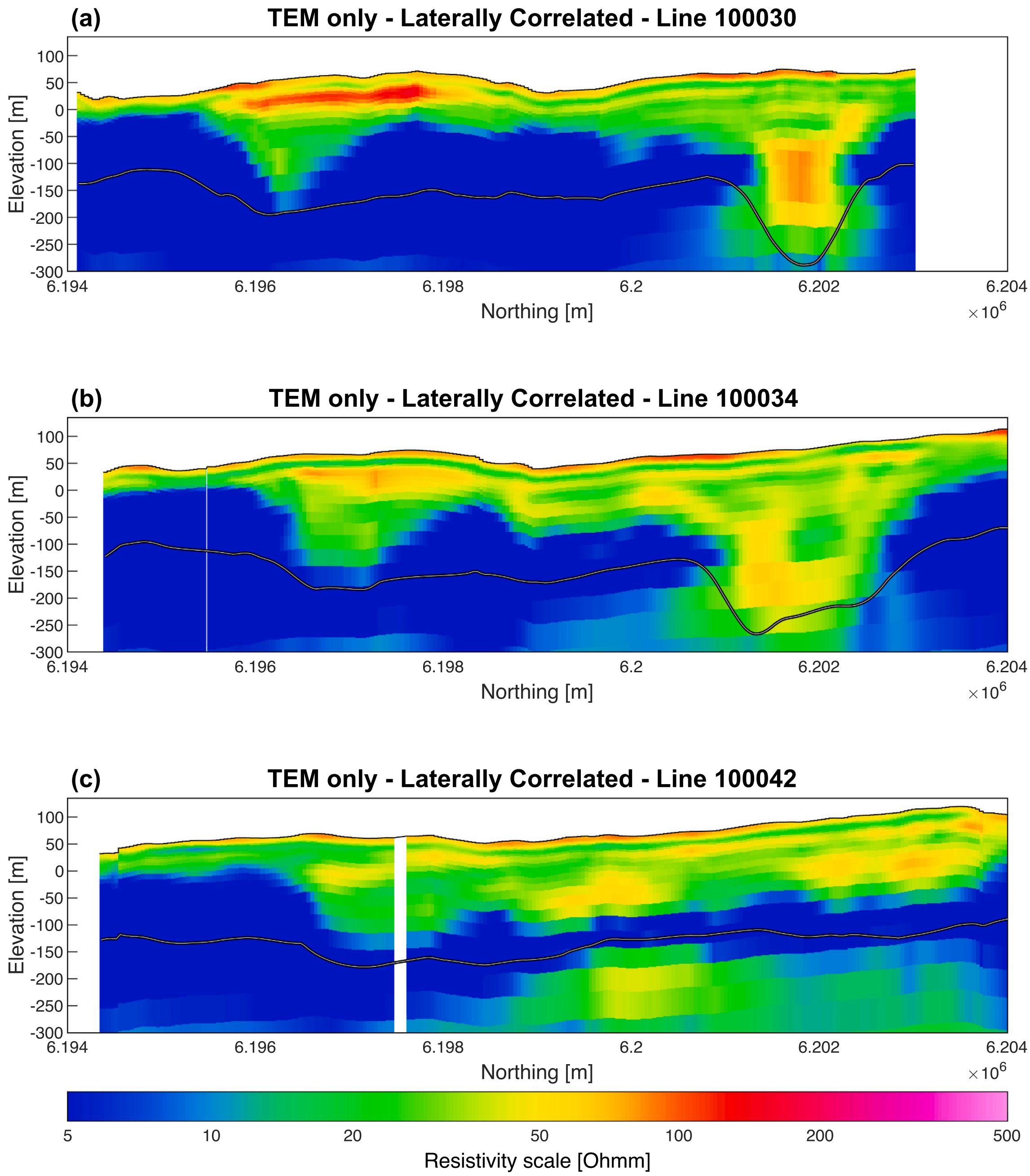

Fig. 5. The model sections of the TEM only laterally correlated inversions. The Easting locations of the three lines are (from top to bottom): E: 554,800 m, E: 555,600 m, and E: 557,200 m. The white lines with black edges indicate the depth of information (DOI).

eastern side of the survey area. Also plotted in Fig. 8 are the error-weighted total residuals of the TEM inversion with TEM data alone and the TEM residuals of the joint inversion models. As can be seen the two maps are quite similar with only small changes within small areas. The same picture emerges when looking at the corresponding residuals of the PACES alone and the PACES residuals of the joint inversion models (not shown here): they are practically similar. These results indicate that the increased complexity of the joint inversion models is not contradicted by the any of the data sets.

5.4. The issue with joint inversion of galvanic (PACES) and inductive (TEM) data

Beside the relative weights of the TEM and PACES models, there is one more issue that warrants some attention. When comparing inversion results from galvanic (PACES) and inductive (TEM) data within the same area, it is a general experience that the galvanic models will have a higher resistivity within those parts of the model where their sensitivity lies, in this case the more near-surface parts of model. This is most often taken to be an effect of (macro-)anisotropy: Galvanic data are sensitive to the geometric mean of the vertical and horizontal resistivities, whereas inductive data are sensitive to the horizontal resistivity only (Christensen, 2000). The question is whether this should preclude a joint inversion of galvanic and inductive data, or whether some sort of modification of the galvanic resistivities is necessary. It is certainly an issue that must be investigated. Does the joint inversion of TEM data with the PACES information distort the final TEM models in an unwanted way?

To cast some light on the problem, a depth interval where both the galvanic and inductive data would have a reasonable resolution was

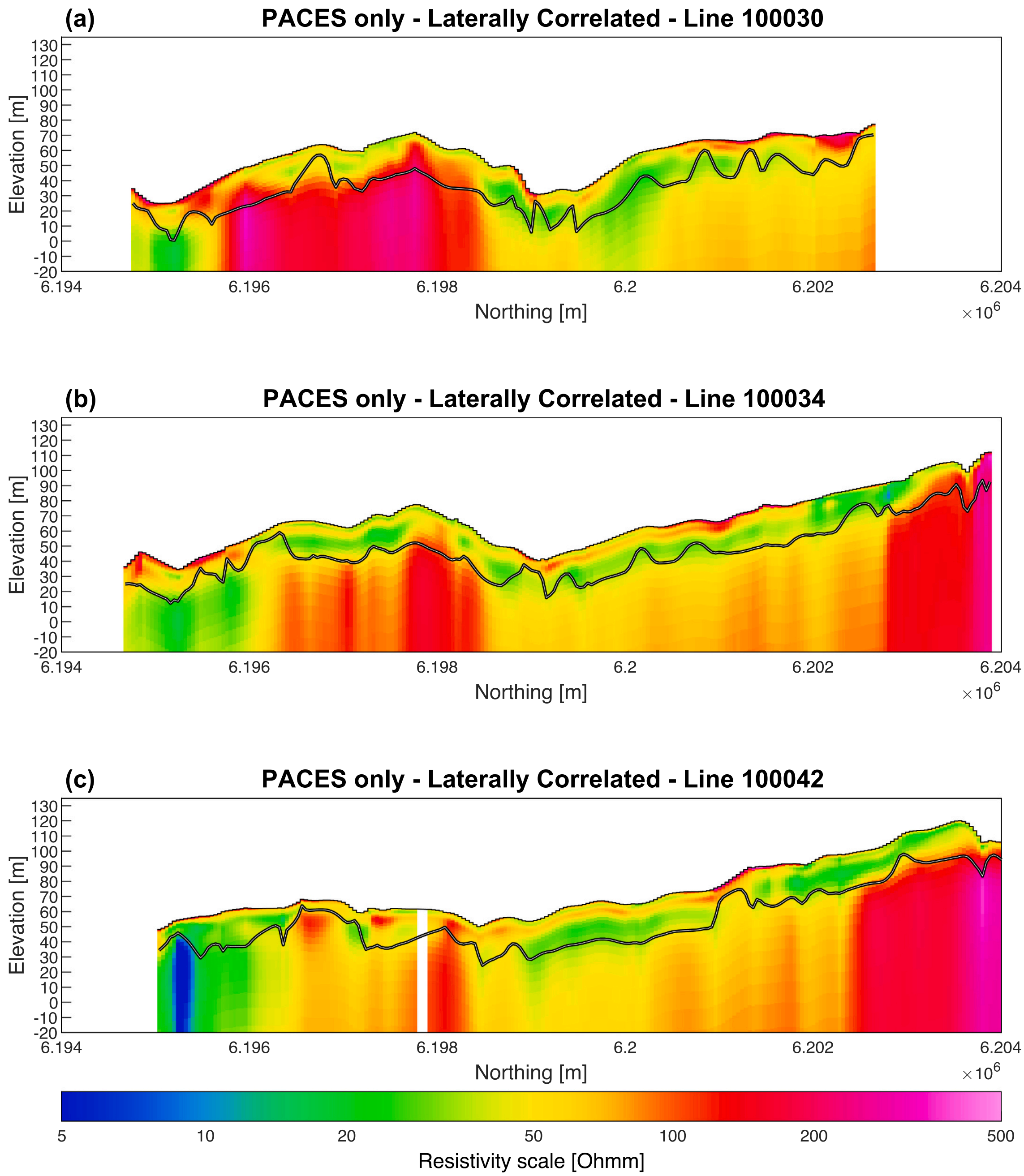

Fig. 6. The model sections of the PACES only laterally correlated inversions. The Easting locations of the three lines are (from top to bottom): E: 554,800 m, E: 555,600 m, and E: 557,200 m. The white lines with black edges indicate the depth of information (DOI).

chosen, namely layers 12–14, i.e. the depth interval from 8.96 to 14.92 m. Fig. 9 shows a crossplot of the mean resistivities: exp.($<\log \rho>$) from the TEM and the PACES data calculated by interpolating the PACES values to the TEM positions and subsequently culling the points outside of the convex hull of the PACES data and the points where the TEM position is more than 50 m from an original PACES data position. It is seen that the PACES and TEM mean resistivities are quite similar. Fig. 9 also shows the ratio between the PACES resistivity and the TEM resistivity, i.e. the coefficient of (macro-)anisotropy, and a histogram of its logarithm. Further, the statistical measures of these terms is listed in the table in Fig. 9. It is seen that the standard deviation of the various measures is considerably greater than the values predicted if the mapping was an identity mapping, meaning that, within the statistical uncertainties, the TEM and PACES resistivities must be regarded as being the same. There is thus no impediment to performing a joint inversion.

This is confirmed by comparing the model sections of the TEM inversions of line 100034 in Figs. 5 and 7. It is seen that the joint inversion of the TEM data with PACES - as expected - only has an influence in the very top of the model and that it does not distort the resistivity distribution in the middle or deeper parts. This is actually the desirable - and expected - outcome of the joint inversion, and supports a justification of the joint inversion efforts.

It is the similarity between the resistivity regimes of the TEM and PACES inversion models that justifies the approach to joint inversion taken here. If, taking uncertainties into account, there had been an appreciable difference between the two regimes, a joint inversion would have to be conducted with the coefficient of anisotropy included in the model space (Christensen, 2000). This would require a selection of the TEM and PACES data so that only those data sets that have approximately the same location will be jointly inverted.

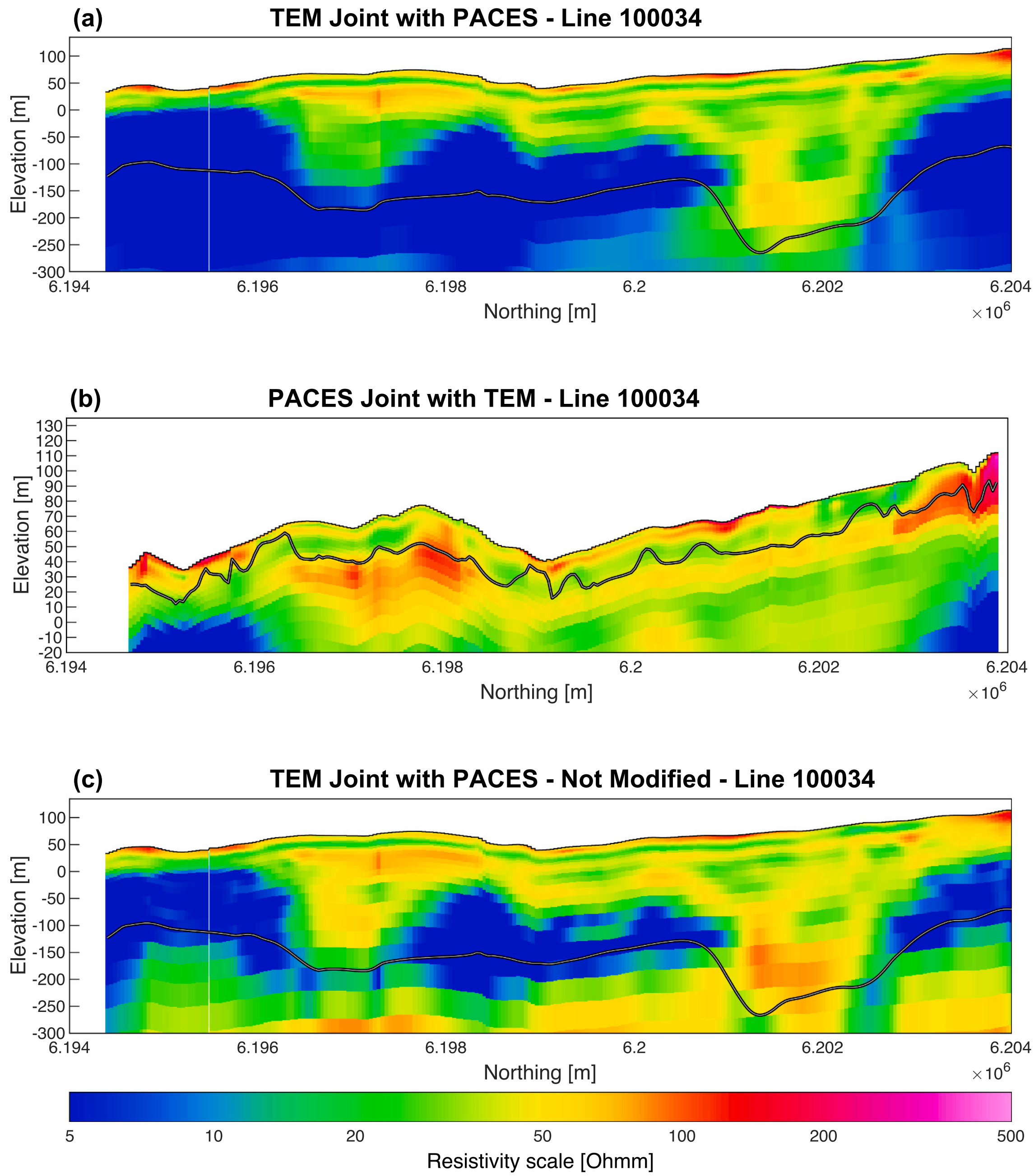

Fig. 7. (a): The model section of line 100,034 of the TEM models from the joint inversion of TEM and PACES data. (b): The model section of line 100,034 of the TEM models from the joint inversion of TEM and PACES data. (c): Same as top frame, but without the down-weighting of the deeper parts of the PACES models before correlation.

6. Conclusions

This paper explores the potential of joint inversion of airborne and ground based data in the Egebjerg survey area, Denmark, where airborne transient electromagnetic data collected with the SkyTEM system have been jointly inverted with Pulled Array Continuous Electrical Sounding (PACES) ground based data. The data were collected as part of the Danish National Groundwater mapping project, and the results of the inversions clearly revealed the buried valleys that are known to be potentially the best aquifers in this part of the country. As intended, including the PACES data in a joint inversion with the TEM data improved the resolution of the near-surface parts of the model in the depth interval 0 -30 m.

Two issues that often arise in joint inversion efforts were addressed. There is a scale difference in the resolution capabilities of the two data sets, with PACES results being reliable only in the top ~30 m of the model, while the TEM data offered resolution to considerably larger depth. This necessitated a down-weighting of the PACES models below the depth of investigation of ~30 m before correlation with the TEM inversion results.

The other issue to be addressed is the fact that galvanic (PACES) and inductive (TEM) data are sensitive to different measures of the subsurface resistivity, the former sensing the geometric mean of the vertical and horizontal resistivity and the latter the horizontal resistivity only. Comparing the mean resistivities of the two methods in a representative depth interval, it was found that the PACES mean resistivity was a factor of ~1.3 higher than the TEM resistivity. However, the joint inversion skewed neither the final PACES model nor the final TEM models of the

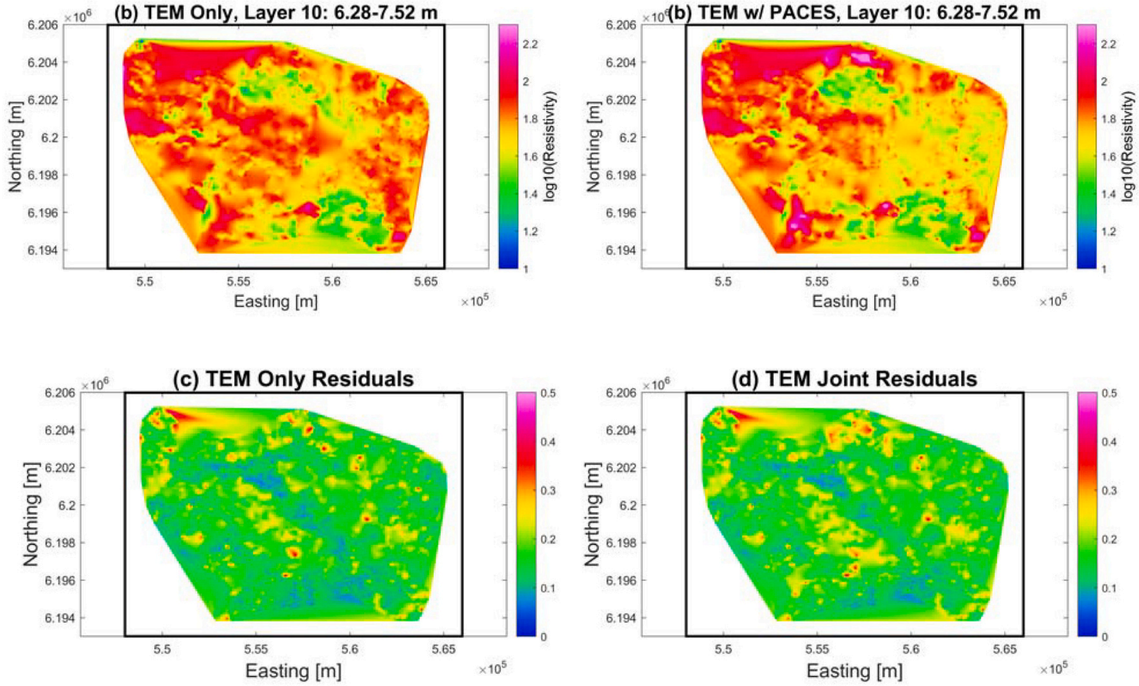

Fig. 8. Maps of the resistivity of layer 10 of the TEM models and the inversion residuals. (a): TEM data alone. (b): Joint inversion of the TEM and PACES data. (c) Inversion residuals of TEM data alone. (d) Residuals of TEM Joint inversions.

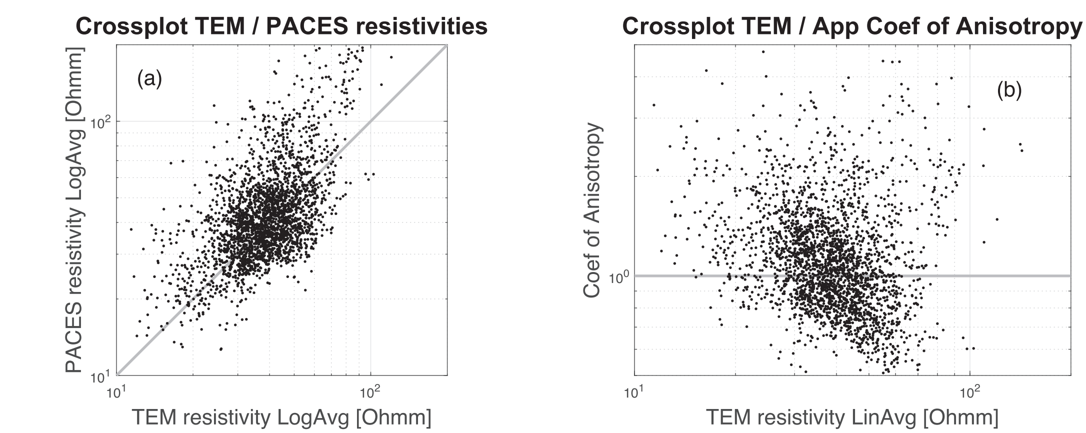

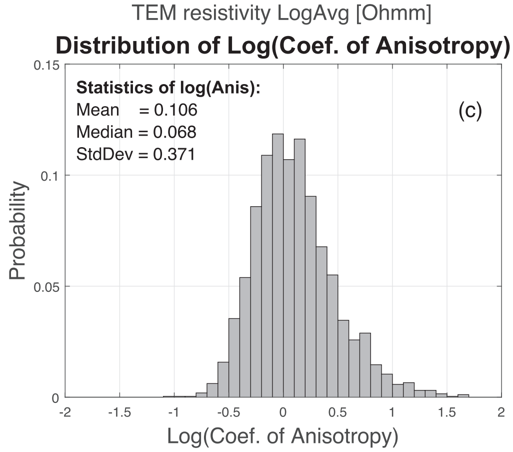

	TEM	PACES	Anis	log(Anis)
Mean	40.539	48.355	1.199	0.106
Median	38.843	40.254	1.071	0.068
StdDev	13.78	33.3	0.536	0.371

Fig. 9. (a): Crossplot of the PACES mean resistivity as a function of the TEM mean resistivity in the depth interval ~9-15m. The mean is calculated as exp.(< log ρ>). (b): Crossplot of the ratio between PACES mean resistivity and TEM mean resistivity, i.e. the coefficient of anisotropy. In all three plots, the thick gray line indicates the identity mapping. (c): Distribution of log (coefficient of anisotropy) with its statistics. The table displaying the statistics of all plot frames.

joint inversion, which is taken as an indication that a joint inversion is justified.

Author statement

Niels B. Christensen: Conceptualisation, Methodology, Software, Supervision, Writing, and Editing. Juletta Christensen: Reviewing. Ingelise Møller: Data Curation.

Declaration of Competing Interest

The author is not aware of any conflicts of interest in relation to this paper.

Acknowledgments

This work is part of the RESPROB project: Probabilistic Geo-modelling of Groundwater Resources financed by The Independent Research Fund, Denmark, 2017.

The data used in this paper are open-source and were kindly retrieved from the GERDA data base.

https://eng.geus.dk/products-services-facilities/data-and-maps/national-geophysical-database-gerda by Ingelise Møller, GEUS, and supplemented with SkyTEM's data report made available by Per Gisselø (Alectia et al., 2008; SkyTEM, 2007) (Grant number: #7017-00160B).

References

Albouy, Y., Andrieux, P., Rakotondrasoa, G., Ritz, M., Descloitres, M., Join, J.-L., Rasolomanana, E., 2001. Mapping coastal aquifers by joint inversion of DC and TEM soundings -three case histories. Ground Water 39, 87–97. https://doi.org/10.1111/j.1745-6584.2001.tb00354.x.

Alectia, Miljøministeriet, Aarhus, Miljøcenter, November 2008. SkyTEM kortlæ gning ved Hovedgård/Egebjerg. Databehandling og geofysisk tolkning (Version 1 11.11.2008. Sagsnummer W01843. Projektleder: FFP. Udarbejdet af: HNI. Godkendt af: FFP. In Danish only).

Auken, E., Christiansen, A.V., Fiandaca, G., Schamper, C., Behroozmand, A.A., Binley, A., Nielsen, E., Efferso, F., Christensen, N.B., Sørensen, K.I., Foged, N., Vignoli, G., 2015. An overview of a highly versatile forward and stable inverse algorithm for airborne, ground-based and borehole electromagnetic and electric data. Explor. Geophys. 2015, 223–235.

Bai, P., Vignoli, G., Hansen, T.M., 2021. 1D stochastic inversion of airborne time-domain electromagnetic data with realistic prior and accounting for the forward modeling error. Remote Sens. 2021, 3881. https://doi.org/10.3390/rs13193881.

Christensen, N.B., 2000. Difficulties in determining of electrical anisotropy in subsurface investigations. Geophys. Prospect. 48, 1–19.

Christensen, N.B., 2016a. Strictly horizontal lateral parameter correlation for 1D inverse modelling of large data sets. Near Surf. Geophys. 14, 391–399. https://doi.org/10.3997/1873-0604.2016028.

Christensen, N.B., 2016b. Fast approximate 1D modelling and inversion of transient electromagnetic data. Geophys. Prospect. 64, 1620–1631. https://doi.org/10.1111/1365-2478.12373.

Christensen, N.B., 2021. Resolution Attributes for Geophysical Inversion Models. Depth of Investigation and Novel Measures (Submitted to Near Surface Geophysics. In review).

Christensen, N.B., Lawrie, K., 2018. A novel approach to comparing AEM inversion results with borehole conductivity logs. Explor. Geophys. 49 (3), 309–322. https://doi.org/10.1071/EG17029.

Christensen, N.B., Tølbøll, R.J., 2009. A lateral model parameter correlation procedure for one-dimensional inverse modelling. Geophys. Prospect. 57, 919–929. https://doi.org/10.1111/j.1365-2478.2008.00756.x.

Christiansen, A.V., Auken, E., Foged, N., Sørensen, K.I., 2007. Mutually and laterally constrained inversion of CVES and TEM data: a case study. Near Surf. Geophys. 2007, 115–123.

Fernando, A., Santos Monteiro, F.A.S., Hesham, M., El-Kaliouby, 2010. Comparative study of local versus global methods for 1D joint inversion of direct current resistivity and time-domain electromagnetic data. Near Surf. Geophys. 8, 135–143. https://doi.org/10.3997/1873-0604.2009056.

Haroon, A., Adrian, J., Bergers, R., Gurk, M., Tezkan, B., Mammadov, A.L., Novruzov, A. G., 2015. Joint inversion of long-offset and central-loop transient electromagnetic data: Application to a mud volcano exploration in Perekishkul, Azerbaijan. Geophys. Prospect. 63, 478–494. https://doi.org/10.1111/1365-2478.12157.

Inman Jr., J.R., Ryu, J., Ward, S.H., 1975. Resistivity inversion. Geophysics 38, 1088–1108.

Jørgensen, F., Møller, R.R., Sandersen, P.B.E., Nebel, L., 2010. 3D geological modelling of the Egebjerg area, Denmark, based on hydrogeophysical data. © GEUS, 2010. Geol. Surv. Denmark Greenland Bull. 20, 27–30. Open Access. www.geus.dk/publications/bull.

Maurer, H., Holliger, K., Boerner, D.E., 1998. Stochastic regularization: smoothness or similarity? Geophys. Res. Lett. 25 (15), 2889–2892.

Meju, M., 2005. Simple relative space–time scaling of electrical and electromagnetic depth sounding arrays: implications for electrical static shift removal and joint DC-TEM data inversion with the most-squares criterion. Geophys. Prospect. 53, 463–479. https://doi.org/10.1111/j.1365-2478.2005.00483.x.

Menke, W., 1989. Geophysical Data Analysis. Discrete Inverse Theory. Academic Press Inc.

Rambøll, 2011. PACES kortlæ gning - Galten, Hårup, Egebjerg, Laurbjerg. Rapport til Miljøministeriet, februar 2011. Additionally: Bilag til Rapport.

Serban, D.Z., Jacobsen, B.H., 2001. The use of broadband prior covariance for inverse palaeoclimate estimation. Geophys. J. Int. 147, 29–40.

Sharma, S.P., Verma, S.K., 2011. Solutions of the inherent problem of the equivalence in direct current resistivity and electromagnetic methods through global optimization and joint inversion by successive refinement of model space. Geophys. Prospect. 59, 760–776. https://doi.org/10.1111/j.1365-2478.2011.00952.x.

SkyTEM kortlægning Egebjerg, 2007. Rådatarapport. SkyTEM Aps.

Sørensen, K.I., 1996. Pulled array continuous electrical profiling. First Break 14 (3), 85–90.

Sørensen, K.I., Auken, E., 2004. SkyTEM - a new high-resolution helicopter transient electromagnetic system. Explor. Geophys. 35, 191–199.

Sudha, Tezkan B., Siemon, B., 2014. Appraisal of a new 1D weighted joint inversion of ground based and helicopter-borne electromagnetic data. Geophys. Prospect. 62, 597–614. https://doi.org/10.1111/1365-2478.12091.

Triantafilis, J., Wong, V., Monteiro Santos, F.A., Page, D., Wege, R., 2011. Modeling the electrical conductivity of hydrogeological strata using joint-inversion of loop-loop electromagnetic data. Geophysics 77 (4). https://doi.org/10.1190/geo2011-0507.1. WB99-WB107.

Vozoff, K., Jupp, D.L.B., 1975. Joint inversion of geophysical data. Geophys. J. Int. 42, 977–991. https://doi.org/10.1111/j.1365-246X.1975.tb06462.x.